

## Polymorphism of Sulfanilamide: (II) Stability Hierarchy of $\alpha$ -, $\beta$ - and $\gamma$ - Forms from Energy Calculations by the Atom-Atom Potential Method and from the Construction of the p, T Phase Diagram

S. Toscani,<sup>1</sup> A. Dzyabchenko,<sup>2</sup> V. Agafonov,<sup>3</sup>  
J. Dugué,<sup>1</sup> and R. Céolin<sup>3,4</sup>

Received June 2, 1995; accepted September 29, 1995

**Purpose.** Sulfanilamide trimorphism was chosen as a model system for comparison between stability hierarchies obtained from lattice-energy calculations with those deduced from the relative locations of the sublimation curves of polymorphs in the sulfanilamide p, T diagram.

**Methods.** The atom-atom potential (AAP) method was used for lattice-energy calculations. The p, T diagram was constructed by using crystallographic and thermodynamic data for  $\alpha$ -,  $\beta$ -, and  $\gamma$ - forms, and by assigning the temperatures of the experimentally observed phase transitions to triple points involving the vapour phase.

**Results.** The hierarchy obtained with the AAP method ( $E_{\alpha} \approx E_{\gamma} \gg E_{\beta}$ ) differs only slightly from that deduced from the positions of the sublimation curves ( $p_{\gamma} > p_{\alpha} > p_{\beta}$ ) in the p, T diagram at room temperature. No stable phase region was found for form  $\alpha$ . Thus it is really monotropic.

**Conclusions.** Provided enthalpy and volume changes at the transitions are accurate enough, it is possible to draw a p, T diagram that accounts for the stability hierarchy of polymorphs.

**KEY WORDS:** atom-atom potential method; polymorphism; monotropy; sulfanilamide.

### INTRODUCTION

Ostwald first showed that polymorphs stabilities are related to their vapour pressures, the lower the pressure the stabler the form, and to the stability hierarchy of the melting triple points  $s_i$ -l-v (l = liquid, v = vapor,  $s_i = i^{\text{th}}$  polymorph of a given body), the higher the melting point the stabler the form. However, these criteria are seldom applied because vapor pressure measurements versus temperature are almost never performed.

Ostwald criteria obviously indicate that stability cannot be taken as an absolute concept. However reticular energy

values, calculated from crystallographic data, provide us with stability hierarchies which do not take temperature and pressure effects into account.

### MATERIALS AND METHODS

#### Energy Calculations and Crystal Packings Comparison

In the AAP method (1), the crystal energy is expressed as the sum of the interatomic energies of a molecule and its surroundings. Because the molecules are linked through hydrogen bonding, we have performed a comparative study of three kinds of intermolecular potentials: MCMS (2), HHL (3), and HHL/CNDO/2. Parameter values of the atom-atom potential for sulfur were taken from ref. (4), and initial data for molecules and lattices from crystal structures (5,7). The PMC program (8) was used for calculations (lattice parameters and molecular orientations were allowed to vary for a fixed crystal symmetry).

For further comparisons, we have used a method (9), in which the graph-set,  $G^a_d(r)$ , is specified using the pattern designator G, its degree r (number of atoms in a ring or in the repeat length in a chain), the numbers d and a of donors and acceptors, respectively. G is identified by the letter C (infinite chain), D (definite chain), R (ring) or S (intramolecular ring).

#### p, T Diagram

The p, T diagram may be constructed by using topological rules (10), and the Clapeyron relation between entropy ( $\Delta S$ ) and volume ( $\Delta V$ ) changes at any phase transition. Three items have to be reminded:

i/ When DSC measurements are performed on samples in closed pans, transitions occur in the presence of a vapour phase which saturates the dead volume inside the pans. It ensues that the onset temperatures of the endothermal effects have to be attributed to triple points involving the vapour phase v.

ii/ Melting triple points  $s_i$ -l-v are situated on a unique boiling curve l-v. We assume that this rule thermodynamically defines polymorphism. These points follow one another, so that their stabilities decrease as temperature decreases (Fig. 1).

iii/ The Le Chatelier's principle may be used in order to localize the stability domains of two polymorphs, with respect to their equilibrium curve:  $\Delta H_{s_i \rightarrow s_j} > 0$  (or  $\Delta H_{s_j \rightarrow s_i} < 0$ ) indicates that the  $s_j$  domain is stabler than the  $s_i$  one at high temperature.

### RESULTS AND DISCUSSION

#### Energy Calculations and Crystal Packings Comparison

Although a large excess in the coulombian energy leading to an overestimated c-value only indicates that the HHL-estimated partial charges are not appropriate, results given in Table I show that, whatever the potential used, the  $\beta$ - form is the stabler one, and that, for  $\alpha$ - and  $\gamma$ - forms, energies  $E_{\alpha}$  and  $E_{\gamma}$  are very similar.  $E_{\gamma}$  is found slightly lower than  $E_{\alpha}$ , but this is not significative because of the low difference

<sup>1</sup> Laboratoire de Chimie Physique et Chimie Minérale, Faculté des Sciences Pharmaceutiques et Biologiques, 4, Avenue de l'Observatoire, 75006 Paris, France.

<sup>2</sup> Karpov Institute of Physical Chemistry, Obukha Street, 10, 107120 Moscow, Russia.

<sup>3</sup> Laboratoire de Chimie Physique, Faculté de Pharmacie, 31, Avenue Monge, 37200 Tours, France.

<sup>4</sup> To whom correspondence should be addressed.

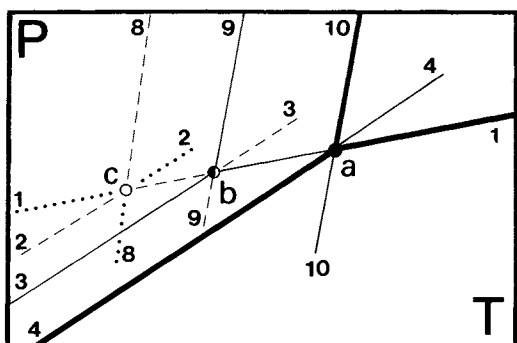


Fig. 1. Stability hierarchy along the  $l$ - $v$  equilibrium curve in the case of trimorphism (for identification of triple points and of two-phase equilibrium curves, see Fig. 4). Triple points: black = stable; black and white = metastable; white = supermetastable. Two-phase equilibrium lines: thick = stable; thin = metastable; dashed = supermetastable; dotted = hypermetastable. Around each triple point, the two-phase equilibrium curves do radiate so that higher and lower stabilities alternate (10).

between the experimental and calculated data. The hierarchy  $E\beta < E\gamma < E\alpha$ , which is the same as the density hierarchy ( $d\beta > d\gamma > d\alpha$ ), obeys the rule according to which the densest form is the stablest one. However, such an agreement results mostly from the AAP method itself, although the electrostatic contribution would invalidate the rule.

Crystal structures show that packings are due to N-H donors and S = O acceptors which link the molecules by means of three-dimensional N-H . . . O = S hydrogen-bond networks. By only considering the N . . . O distances lower than 3.11 Å, the  $\beta$ -form packing is observed as a three-dimensional network (Fig. 2A). It is very different from those in  $\alpha$ - and in  $\gamma$ - form (Fig. 2B and C). They are also three-dimensional networks, but considering the same limit, they are found consisting of layers approximately parallel to plane (010) in  $\alpha$ - form and to (100) in  $\gamma$ - form.

The hydrogen bond network (primary ( $N_1$ ) + secondary ( $N_2$ ) networks) is stated as a series of graph-sets: for  $\alpha$ -form,  $N_1 = C(8) C(4) R^2_2(8)$ ,  $N_2 = C^2_2(6) R^6_6(20)$ , for  $\gamma$ -form,  $N_1 = C(4) R^2_2(8)$ ,  $N_2 = C^2_2(6) R^6_6(20)$ , and for  $\beta$ -form,  $N_1 = C(8) C(4)$ ,  $N_2 = R^3_4(22)$ .

The networks are represented in Fig. 3A, B and C.

These assignments show that the difference between similar  $\alpha$ - and  $\gamma$ -forms mainly consists in the presence of C(8) chains in  $\alpha$ -form. This result may account for the low difference in energy calculated between both forms, but it disagrees with the high value of the enthalpy change at the  $\alpha$ - $\gamma$  transition (Table 2).

### Sulfanilamide p, T Diagram

Experimental and calculated data are collected in Table 2. The inequality  $V_\alpha > V_\gamma > V_\beta$  is corroborated by grinding and compression experiments: forms  $\alpha$  (11) and  $\gamma$  (12) transform into form  $\beta$ , as pressure increases. We have observed that form  $\alpha$  transformed into form  $\gamma$  by crushing up.

In the case of trimorphism, three triple points with two common phase are situated on the two-phase equilibrium curve involving these phases (10). Inset A in Fig. 4 shows the relative positions of 5 experimental triple points over the 10

Table I.  $E_T$  (kcal · mol<sup>-1</sup>): Reticular Energy,  $E_C$  (kcal · mol<sup>-1</sup>): Electrostatic Contribution, a, b, c (Å) and  $\beta$  (°): Lattice Parameters, d (g · cm<sup>-3</sup>): Density, S(Å): Overall Shift of the Molecular Center in the Calculated Structure with Respect to the X-Ray One;  $\Omega$  (°): Turn Angle Defining the Overall Rotation of the Molecule with Respect to Its Position in the X-Ray Structure

	X-rays	MCMS	HHL	HHL/ CND0/2
$\alpha$ -FORM (orthorhombic, Pbca, Z = 8)				
$E_T$		-21.52	-25.11	-19.15
$E_C$		-1.76	-12.07	-1.80
a	5.650	5.45	4.8	5.93
b	18.509	17.82	15.86	17.31
c	14.794	15.39	23.11	15.64
d	1.478	1.53	1.29	1.42
S		0.60	1.50	0.64
$\Omega$		9.2	30.2	11.9
$\beta$ -FORM (monoclinic, P2 <sub>1</sub> /c, Z = 4)				
$E_T$		-24.07	-27.05	-20.40
$E_C$		-3.78	-11.20	-2.38
a	8.975	7.79	8.57	8.97
b	9.005	8.46	8.93	8.99
c	10.039	12.11	10.91	10.92
$\beta$	111.43	115.9	107.3	117.5
d	1.514	1.59	1.42	1.46
S		0.07	0.43	0.32
$\Omega$		25.8	13.5	12.5
$\gamma$ -FORM (monoclinic, P2 <sub>1</sub> /c, Z = 4)				
$E_T$		-22.54	-25.17	-19.39
$E_C$		-2.71	-11.86	-1.97
a	7.949	7.72	7.90	7.90
b	12.944	13.02	14.18	13.00
c	7.789	7.36	8.00	8.02
$\beta$	106.50	100.6	101.6	106.0
d	1.488	1.57	1.30	1.44
S		0.80	0.69	1.03
$\Omega$		25.0	13.8	20.4

possible ones. Such a figure had been drawn, neither taking the vapour phase nor the metastability hierarchy into account, by Sekiguchi (13) who suggested that the  $\alpha$ - $\beta$  transition might occur at ca 154 K. This disagrees with low-temperature experiments (14) and with the following observations. The difference between T( $\alpha$ - $\gamma$ - $v$ ) and T( $\beta$ - $\gamma$ - $v$ ) is 10° at ca 386 K, and that for triple points  $\alpha$ - $l$ - $v$  and  $\beta$ - $l$ - $v$  is 6° at ca 426 K. Hence,  $\alpha$ - $v$  and  $\beta$ - $v$  curves, considered as straight lines, cross at ca 486 K, temperature of triple point  $\alpha$ - $\beta$ - $v$ . This result indicates that this point is situated at high temperature. It also agrees with the endothermic character of the  $\beta$ -> $\alpha$  transition, indicating that the  $\alpha$ - form domain would be placed at temperatures higher than that for form  $\beta$ .

The  $\beta$ - $\gamma$  and  $\alpha$ - $\gamma$  equilibrium curves converge towards the  $\alpha$ - $\beta$ - $\gamma$  triple point. Since their slopes  $dp/dT$  have opposite signs (Table 2), this point is located in the low-pressure region. It is metastable because it is situated on the metastable extension of the  $\beta$ - $\gamma$  curve. By assuming  $p = 0$  at points  $\alpha$ - $\gamma$ - $v$  and  $\beta$ - $\gamma$ - $v$ , the calculated coordinates of triple point  $\alpha$ - $\beta$ - $\gamma$  are T = 384 K and  $p = -17$  MPa. The slope of the  $\alpha$ - $\beta$  equilibrium curve may be calculated by using the tempera-

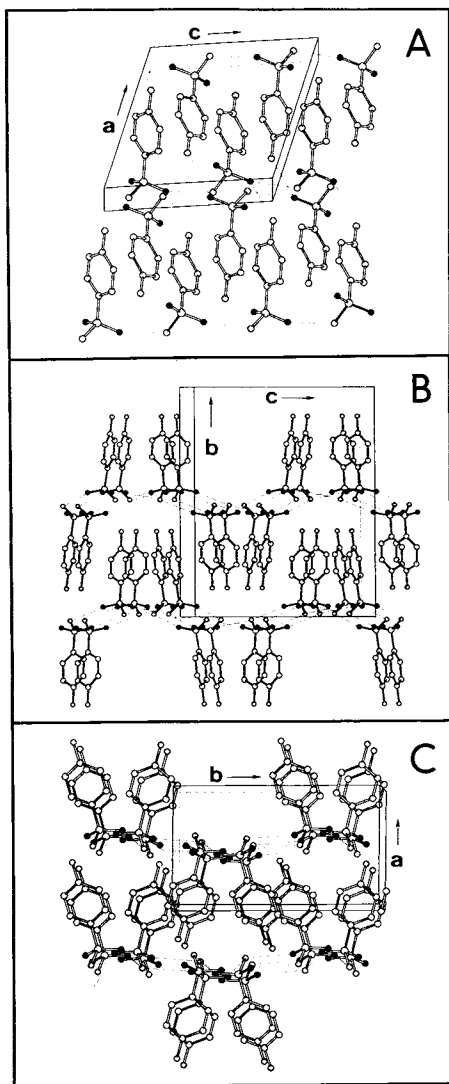


Fig. 2. Molecular packings (with unit-cells) in sulfanilamide polymorphs (H-atoms omitted). A:  $\beta$ -form, B:  $\alpha$ -form, C:  $\gamma$ -form. Thin dotted lines = hydrogen bonds. Dark circles = oxygen atoms.

ture of the  $\alpha$ - $\beta$ - $\gamma$  triple point, which it crosses. This value (Table 2) may be used to estimate the temperature of triple point  $\alpha$ - $\beta$ - $\nu$ . Considering that curve  $\alpha$ - $\beta$  may be described by  $p + 17 = 0.114 (T - 384)$ ,  $p = 0$  entails  $T = 533$  K.

Since the volume variations at melting are not known, triple points  $\alpha$ - $\beta$ - $l$ ,  $\alpha$ - $\gamma$ - $l$  and  $\beta$ - $\gamma$ - $l$  cannot be located at first sight. However,  $\alpha$ - $\beta$ - $l$  has to be on the  $\alpha$ - $\beta$  curve that links  $\alpha$ - $\beta$ - $\gamma$  and  $\alpha$ - $\beta$ - $\nu$ . The relative stabilities of the curves that converge to these points are detailed in Fig. 4, which shows that the portion of curve  $\alpha$ - $\beta$  between these points is supermetastable when crossing  $\alpha$ - $\beta$ - $\nu$ , and that it is hypermetastable when crossing  $\alpha$ - $\beta$ - $\gamma$ . Therefore, point  $\alpha$ - $\beta$ - $l$  on curve  $\alpha$ - $\beta$  has to be between  $\alpha$ - $\beta$ - $\gamma$  and  $\alpha$ - $\beta$ - $\nu$ , where the metastability degree of the  $\alpha$ - $\beta$  equilibrium changes. It comes that curves  $\alpha$ - $l$  and  $\beta$ - $l$  converge at lower pressures, whatever their slopes, at a temperature which is in the range 423–429 K. For the  $p$ , $T$  diagram to be completed, stable curves  $\beta$ - $\gamma$  and  $\gamma$ - $l$  have been drawn so that they cross in the high-pressure region at the stable  $\beta$ - $\gamma$ - $l$  triple point. In such a case, the

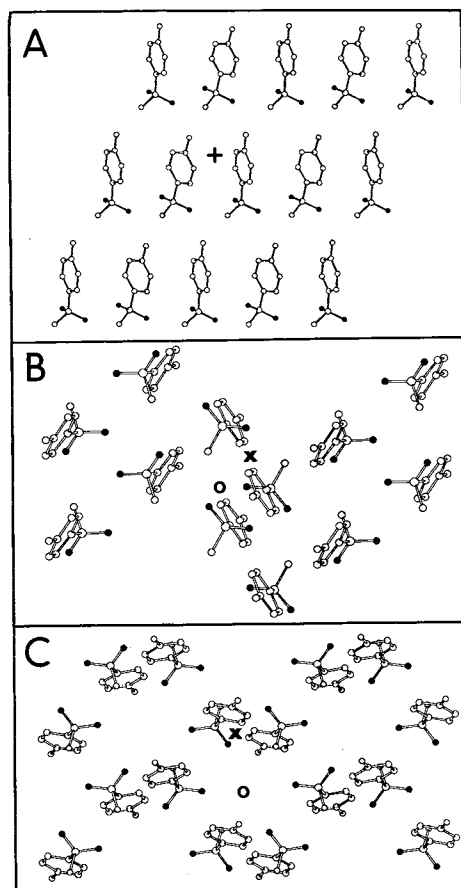


Fig. 3. Hydrogen-bond (thin dotted lines) motifs in sulfanilamide polymorphs (H-atoms omitted). A:  $\beta$ -form, B:  $\alpha$ -form, C:  $\gamma$ -form. Motifs: + =  $R^3_4(22)$ , x =  $R^2_2(8)$ , o =  $R^6_6(20)$ .

stable  $\gamma$ -phase domain is triangular. Then the tenth triple point,  $\alpha$ - $\gamma$ - $l$ , would be situated at lower pressures on the metastable portion of curve  $\alpha$ - $\gamma$ .

## CONCLUSIONS

For sulfanilamide  $\alpha$ -,  $\beta$ - and  $\gamma$ - forms, the stability hierarchy can be deduced from the relative positions of their sublimation curves. At  $T < 381$  K, the inequality  $p\beta < p\alpha <$

Table II. Data Used for the Drawing of the Sulfanilamide  $p$ ,  $T$  Diagram

FORM ( $M = 172.2$ )	$\alpha$	$\beta$	$\gamma$
Tfus/K	423	429	438
Associated triple point	$\alpha - l - \nu$	$\beta - l - \nu$	$\gamma - l - \nu$
$V/\text{cm}^3 \cdot \text{g}^{-1}$	0.6764	0.6604	0.6719
TRANSITION	$\alpha \rightarrow \beta$	$\beta \rightarrow \gamma$	$\alpha \rightarrow \gamma$
T/K	ca 500 K	391	381
Associated triple point	$\alpha - \beta - \nu$	$\beta - \gamma - \nu$	$\alpha - \gamma - \nu$
$\Delta H/J \cdot \text{g}^{-1}$	-0.7	+10.9	+10.2
$\Delta V/\text{cm}^3 \cdot \text{g}^{-1}$	-0.016	+0.0115	-0.0045
$(dp/dT)/\text{MPa} \cdot \text{K}^{-1}$	+0.175	+2.42	-5.95

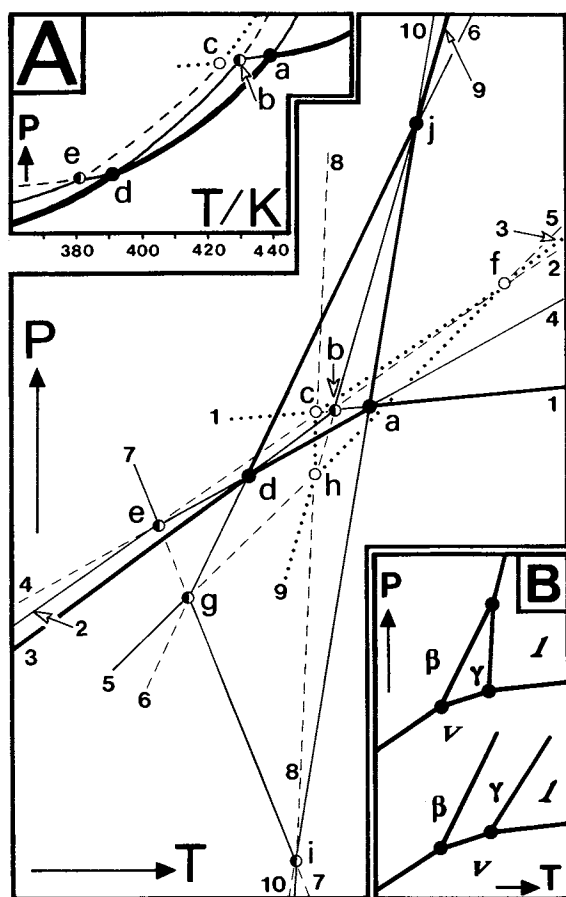


Fig. 4. Sulfanilamide p, T phase diagram. Relative stabilities shown as in Fig. 3. Triple points: a:  $\gamma$ - $l$ - $v$ , b:  $\beta$ - $l$ - $v$ , c:  $\gamma$ - $l$ - $v$ , d:  $\beta$ - $\gamma$ - $v$ , e:  $\alpha$ - $\gamma$ - $v$ , f:  $\alpha$ - $\beta$ - $v$ , g:  $\alpha$ - $\beta$ - $\gamma$ , h:  $\alpha$ - $\beta$ - $l$ , i:  $\alpha$ - $\gamma$ - $l$ , j:  $\beta$ - $\gamma$ - $l$ . Two-phase equilibrium curves: 1:  $l$ - $v$ , 2:  $\alpha$ - $v$ , 3:  $\beta$ - $v$ , 4:  $\gamma$ - $v$ , 5:  $\alpha$ - $\beta$ , 6:  $\beta$ - $\gamma$ , 7:  $\alpha$ - $\gamma$ , 8:  $\alpha$ - $l$ , 9:  $\beta$ - $l$ , 10:  $\gamma$ - $l$ . Inset A: location of the experimentally observed triple points. Inset B: representation of the stable phase regions. Upper part: low pressure enantiotropy of form  $\gamma$ . Lower part: overall enantiotropy of form  $\gamma$ .

$p\gamma$  indicates that  $\beta$  is stabler than  $\alpha$ , which is itself stabler than  $\gamma$ . At  $381 < T/K < 391$ ,  $p\beta < p\gamma < p\alpha$  indicates that  $\beta$  remains the stabler form, and that form  $\gamma$  is stabler than form  $\alpha$ . At  $T > 391$  K, the inequality  $p\gamma < p\beta < p\alpha$  indicates that form  $\gamma$  becomes the stabler form, and form  $\alpha$  the less stable one.

Although uncertainties persist about the location of some triple points, no stability region is found for form  $\alpha$ , which only becomes less metastable as temperature increases. Therefore, it is really monotropic (15), whichever temperature and pressure considered.

Also from lattice energy calculations, form  $\beta$  is found to

be the stablest one. The disagreement in metastability between forms  $\alpha$  and  $\gamma$  may be due to the parameters values of the sulfur-sulfur potential, which are less accurately known than those for the other atoms. Anyway, the method followed in drawing the sulfanilamide p, T diagram may be used to validate lattice-energy calculations.

## REFERENCES

1. A. J. Pertsin, and A. I. Kitaigorodskii. The atom-atom potential method, Springer Verlag, N.-Y., USA. (1987).
2. F. A. Momany, L. M. Carruthers, R. F. McGuire, and H. A. Scheraga. Intermolecular potentials from crystal data. III. Determination of empirical potentials and application to the packing configurations and lattice energies in crystals of hydrocarbons, carboxylic acids, amines, and amides. *J. Phys. Chem.* 78:1595-1620 (1974).
3. A. T. Hagler, E. Huler, and S. Lifson. Energy functions for peptides and proteins. I. Derivation of a consistent force field including the hydrogen bond from amide crystals. *J. Am. Chem. Soc.* 96:5319-5327 (1974).
4. D. J. Sandman, A. J. Epstein, J. S. Chickos, J. Ketchum, J. S. Fu, and H. A. Scheraga. Crystal lattice and polarization energy of tetrathiafulvalene. *J. Chem. Phys.* 70:305-315 (1979).
5. B. H. O'Connor, and E. N. Maslen. The crystal structure of  $\alpha$ -sulphanilamide. *Acta Crystallogr.* 18:363-366 (1965).
6. A. M. O'Connell and E. N. Maslen. X-ray and neutron diffraction studies of  $\beta$ -sulphanilamide. *Acta Crystallogr.* 22:134-145 (1967).
7. M. Alléaume. Etude cristallographique de composés sulfamidés. Thèse. Université de Bordeaux (1967).
8. A. V. Dzyabchenko, V. K. Belsky, and P. M. Zorkii. Calculation of optimum molecular packing in crystals in an atom-atom approximation. Algorithm and program for a computer. *Kristallografiya.* 24:221-226 (1979).
9. M. C. Etter, J. C. MacDonald, and J. Bernstein. Graph-set analysis of hydrogen-bond patterns in organic crystals. *Acta Cryst., sect. B: structural science.* B46:256-262 (1990).
10. R. Céolin, S. Toscani, V. Agafonov, and J. Dugué. Phenomenology of polymorphism (I): pressure-temperature representation of trimorphism. General rules. Application to the case of dimethyl 3,6-dichloro-2,5-dihydroxy-terephthalate. *J. Solid State Chem.* 98:366-378 (1992).
11. H. Jünginger. Modifikationsumwandlungen durch mechanische Bearbeitung. 3. Mitteilung: Modifikationsumwandlungen von Sulfanilamid durch Mahlprozesse. *Deutsch Apotheker Zeitung.* 117:456-459 (1977).
12. H. Jünginger. Modifikationsumwandlungen durch mechanische Bearbeitung. 4. Mitteilung: Modifikationsumwandlungen von Sulfanilamid bei der Tablettenkompression. *Pharm. Ind.* 38:724-728 (1976).
13. K. Sekiguchi, Y. Tsuda, and M. Kanke. Dissolution behaviour of solid drugs. VI. Determination of transition temperatures of various physical forms of sulfanilamide by initial dissolution rate measurements. *Chem. Pharm. Bull.* 23:1353-1362 (1975).
14. S. Toscani, S. Thorén, V. Agafonov, R. Céolin, and J. Dugué. Thermodynamic study of sulfanilamide polymorphism: (I) monotropy of the  $\alpha$ -variety. *Pharm. Res.* in press.
15. R. Céolin, S. Toscani, and J. Dugué. Phenomenology of polymorphism (II). Criteria for overall (p,T) monotropy: applications to monochloroacetic acid and to hydrazine monohydrate. *J. Solid State Chem.* 102:465-479 (1993).